

Effect of Phase Change Material on the Performance of a Packed Bed for Cool Latent Heat Storage Systems

Zakareia A. Alarabi¹, Altaher O. Alreda²

^{1,2}Higher Institute of Petroleum Technology, Awbari, LIBYA
Zakareia82@Gmail.Com¹, Redaaltaher708@Gmail.com²

Abstract

This paper introduces a mathematical and numerical analysis of a packed bed containing spherical capsules filled with phase change material (PCM) for latent cool thermal energy storage (TES). The considered bed is the cylindrical tank and containing spherical capsules arranged in a random form. According to the energy balance on the PCM and the heat transfer fluid (HTF), the governing equations and boundary conditions are derived at transient conditions and used a continuous phase model in this model; the spherical capsules are assumed to behave as a continuous medium. The governing equations of the HTF and PCM are discretized using the implicit finite difference approach and central difference approximation. The resulting algebraic equations were solved used MATLAB program. The numerical results are obtained to study the effects of phase change material on the temperature distribution and energy stored in the bed in both charging and discharging modes.

Keywords: Packed bed, Phase change material, Thermal energy storage

1. Introduction

The storage of thermal energy is very important to many engineering applications. TES techniques are known from long time ago, but in latest years, more concern has been paid for the development of TES. Many studies have been done for PCM applications for latent TES, cold energy storage, enhancement of PCM thermal characteristics, and some applications of PCMs for thermal energy management are presented hereafter. Ismail and Henriquez [1] presented a mathematical model for predicting the thermal performance of the cylindrical storage tank containing spherical capsules filled with water as PCM. The results shown that, the effect of varying the entry temperature of the working fluid has a very dominant and strong effect on the solidification time, while varying the temperature from -9 to -15 leads to little variation of the time for complete solidification. In addition, Bilir and Ilken [2] investigated numerically the inward solidification problem of a PCM encapsulated in a cylindrical/spherical container with a third kind of boundary condition and ended up with a correlation which express the dimensionless total solidification time in terms of Stefan number, Biot number and superheat parameter. Moreover, Regin et al. [3] developed a theoretical model for analysis of the behavior of a packed bed consisting of spherical capsules filled with paraffin wax as PCM for latent TES system. A cylindrical storage tank completely filled with PCM capsules. Were observed that the complete solidification time is longer than the melting time, and the capsule with a smaller radius has a significantly higher charging and discharging rates compared to those of larger radius. On the other hand S. Wu [4] presented a mathematical model of the cool TES system using packed bed containing spherical capsules filled with n-tetradecane to predict the thermal behaviour of the system. It was found lower porosity indicates higher cool storage capacity of packed bed, and hence longer time required for complete solidification and melting. The value of cool stored and released rate is much smaller at lower porosity. In addition, Cheralathan et al. [5] investigated

numerically and experimentally a temperature profiles of HTF and PCM at any axial location and studied the influence of porosity during the charging process. The results showed that, for lower porosity, the time averaged internal heat transfer coefficient and heat capacity of storage system are higher and longer time required for freezing the PCM. On the other hand ElGhnam et al. [6] investigated experimental study on the heat transfer during freezing and melting of water inside a spherical capsule of ice storage systems. The results show that the energy recovery ratio is becoming better when using metallic capsules, increasing the capsule size and reducing the HTF volume flow rates, Furthermore Cho and Choi [7] investigated experimentally the thermal characteristics of spherical capsules using n- tetradecane, mixture of n-tetradecane and n-hexadecane and water as PCM, the study gives that the local phase-change temperatures of paraffin in a capsule were different during freezing and melting processes.

2. Physical model

The physical system under study is shown in Figure 1. A cylindrical tank (called packed bed), the packed bed is insulated with polyurethane foams, and has an inner diameter of 1 m, a wall thickness of 0.05 m, and a height of 1.5 m. The PCM is encapsulated in spherical capsules packed randomly in the insulated cylindrical storage tank. Spherical capsules made of polyethylene, has an inner diameter of 0.078 m and a thickness of 0.001 m.

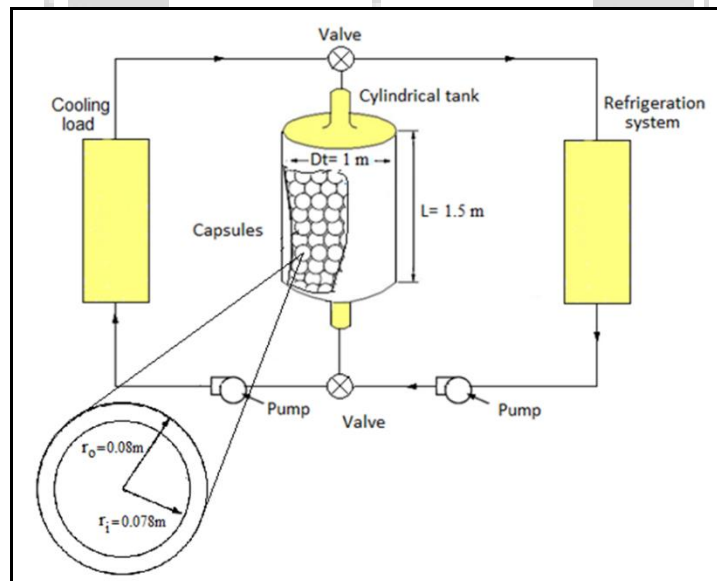


Figure 1 Layout and details of the packed bed cool TES system

In this study, in the charging process, the HTF is charged from the bottom of the cool TES tank upwards, and flows over the spherical capsules in the cool TES tank. The HTF circulation is maintained by using a pump and exchanges energy with the PCM capsules and transfers the heat to the evaporator in a refrigeration system. In this process, PCM in the spherical capsules undergoes sensible cooling of liquid phase, solidification, sensible sub-cooling of solid phase. While in the discharging mode, the refrigeration system is not in operation. The HTF passes through the storage medium from the top of the cool TES tank downwards at temperature higher than the PCM fusion temperature, so heat transfer occurs. Energy released from the storage tank is controlled by flow control valves, and PCM in spherical capsules undergoes sensible heating of solid phase, melting, and sensible heating of liquid phase

3. Mathematical model

The conservation of mass, momentum, and energy can be written as following, respectively:

$$\frac{\partial \rho}{\partial \tau} = -(\nabla \cdot \rho \underline{v}) \quad 1$$

$$\frac{\partial (\rho \underline{v})}{\partial \tau} = -(\nabla \cdot \rho \underline{v} \underline{v}) - \nabla P + \mu \nabla^2 \underline{v} + \rho \underline{g} \quad 2$$

$$\frac{\partial (\rho c_p T)}{\partial \tau} = -(\nabla \cdot \rho c T \underline{v}) + k \nabla^2 T + q''' \quad 3$$

Where (\underline{g}) is acceleration vector, (m/s^2) and (q''') is the heat source or sink in (W/m^3). The charging fluid flow is considered to be incompressible. Therefore, the mass conservation equation becomes:

$$\nabla \cdot \rho \underline{v} = 0 \quad 4$$

The fluid flow is assumed one-dimensional, thus continuity equation, (4) can be integrated to yield:

$$\rho_f (v_f)_y = constant \quad 5$$

in the y-direction a momentum equation reduces to the following form:

$$\left[\rho_f (v_f)_y \right] \frac{d(v_f)_y}{dy} = - \frac{dP}{dy} \quad 6$$

the pressure drop across the packed bed [8] to geometrical parameters as follows:

$$\Delta P = \left[\frac{150 \mu (1 - \varepsilon)^2}{d_o^2 \varepsilon^3} (v_f)_y + \frac{1.75 \rho_f (1 - \varepsilon)}{d_o \varepsilon^3} (v_f)_y^2 \right] L \quad 7$$

The energy balance equation on PCM and HTF can be written based on Shuangmao [4] model as:

$$\rho_f C_f \varepsilon \frac{\partial T_f}{\partial \tau} + \rho_f C_f \varepsilon v_f \frac{\partial T_f}{\partial y} = k_f \varepsilon \frac{\partial^2 T_f}{\partial y^2} + h_e a (\theta - T_f) \quad 8$$

The first term of the left hand side of Eq. (8) represents the rate change of internal energy of HTF, while the second term accounts for energy change due to the HTF flow. The two terms on the right hand represent the heat transfer by conduction and by convection between the HTF and the capsules, respectively. In the solidification stage, the PCM temperature θ should be equal to freezing point (θ_s).

The PCM temperature is also calculated by using energy balance on PCM and HTF.

Liquid phase stage (first stage):

$$\rho_l C_l (1 - \varepsilon) \frac{\partial \theta}{\partial \tau} = h_e a (T_f - \theta) \quad 9$$

Solidification stage (second stage):

$$\rho_s h_i (1 - \varepsilon) \frac{\partial \beta}{\partial \tau} = h_e a (\theta_s - T_f) \quad 10$$

Where L , β and T_m denote latent heat of freezing, solid fraction and freezing temperature, respectively.

Solid phase stage (last stage):

$$\rho_s C_s (1 - \varepsilon) \frac{\partial \theta}{\partial \tau} = h_e a (T_f - \theta) \quad 11$$

Where (ε) is the porosity of the bed, which was calculated using the correlation proposed by Beavers [9]:

$$\varepsilon = 0.4272 - 4.516 \times 10^{-3} \left(\frac{D}{d_o} \right) + 7.881 \times 10^{-5} \left(\frac{D}{d_o} \right)^2 \quad 12$$

And (a) is surface area per unit volume (m^{-1})

$$a = \frac{6(1 - \varepsilon)}{d_o} \quad 13$$

The heat transfer coefficient between the spherical capsules and fluid was developed by Beek [10] for the case of capsules arranged in random form.

$$Nu = 3.22 R_e^{1/3} P_r^{1/3} + 0.117 R_e^{0.8} P_r^{0.4} \quad 14$$

The mean velocity, Reynolds number, Prandtl number of HTF can be obtained respectively from the relations,

$$v_f = \frac{\dot{V}}{\varepsilon A_t} \quad 15$$

$$Re = \frac{v_f \rho d_o}{\mu} \quad 16$$

$$Pr = \frac{c_f \mu}{k_f} \quad 17$$

The heat transfer coefficient is determined from

$$h = \frac{k_f Nu}{d} \quad 18$$

The solid-liquid interface can be calculated as follows,

$$r_p = [(1 - \beta)^{1/3}] \times r_i \quad 19$$

The effective coefficient of heat transfer can be determined from,

$$h_e = \frac{h}{\left(1 + \frac{hr_o(r_o - r_i)}{k_c r_i} + \frac{hr_o^2(r_i - r_p)}{k_s r_i r_p}\right)} \quad 20$$

The cool charge rate during charging process can be represented as,

$$Q_{ch} = \dot{V} \rho_f c_f (T_o - T_{in}) \quad 21$$

The cool charge capacity during charging process can be obtained as,

$$Q_{t, ch} = \int_0^{t_{ch}} Q_{ch} \cdot dt \quad 22$$

The cool discharge rate during charging process can be represented as,

$$Q_{disch} = \dot{V} \rho_f c_f (T_{in} - T_o) \quad 23$$

The cool discharge capacity during charging process can be obtained as,

$$Q_{t, disch} = \int_0^{t_{disch}} Q_{disch} \cdot dt \quad 24$$

4. Boundary and Initial Conditions

The boundary condition can be expressed as follows:

$$T_f(y = 0) = T_{in} \quad \text{for all } \tau$$

And $\frac{\partial T_f}{\partial y}(y = L) = 0 \quad \text{for all } \tau$

The second condition is the initial conditions for the first charging process.

At $T_f(\tau = 0) = T_{in} \quad \text{for } y=0$

$$T_f(\tau = 0) = T_o \quad \text{for } y \neq 0$$

$$\theta(\tau = 0) = T_o \quad \text{for } y \neq 0$$

On the other hand, when the bed is discharged, the boundary condition becomes:

At $T_f(y = 0) = T_o \quad \text{for all } \tau$

And $\frac{\partial T_f}{\partial y}(y = L) = 0 \quad \text{for all } \tau$

And the initial condition, in the discharging process

At $T_f(\tau = 0) = T_o \quad \text{for } y=0$

$$T_f(\tau = 0) = T_{in} \quad \text{for } y \neq 0$$

$$\theta(\tau = 0) = T_{in} \quad \text{for } y \neq 0$$

5. Numerical method

The coupled (HTF) and (PCM) energy equations, along with their initial and boundary conditions, are discretized using implicit finite difference approach and central difference approximation. The packed bed is divided into M layers along the axial direction. The space step and time step are (Δx) and $(\Delta \tau)$.

The discretized equations were solved by MATLAB program. The discretized equations (9) and (11) can be written as following,

$$\theta_i^{n+1} = \frac{\theta_i^n + \omega_i^n \Delta \tau T_i^{n+1}}{1 + \omega_i^n \Delta \tau} \quad 25$$

Where

$$\omega_i^n = \frac{h_{ei}^n a}{\rho_l C_l (1 - \varepsilon)} \quad \text{Liquid phase}$$

$$\omega_i^n = \frac{h_{ei}^n a}{\rho_s C_s (1 - \varepsilon)} \quad \text{Solid phase}$$

With Phase change stage (10):

$$\beta_i^{n+1} = \beta_i^n + \omega_i^n \Delta \tau (\theta_s - T_i^{n+1}) \quad 26$$

Where

$$\omega_i^n = \frac{h_{ei}^n a}{\rho L (1 - \varepsilon)}$$



ρ is equal to ρ_s for charging and ρ_l for discharging. Substituting equations (21) and (22) into finite difference form of equation (8), yields the following general expression for the (HTF)

$$(A - B)T_{i+1}^{n+1} + (1 + 2B + C_i^n)T_i^{n+1} + (-A - B)T_{i-1}^{n+1} = T_i^n + C_i^n \theta_i^n \quad 27$$

Where

$$A = \frac{v_f \Delta \tau}{2 \Delta x} \quad 28$$

$$B = \frac{k_f \Delta \tau}{\rho_f C_f \Delta x^2} \quad 19$$

$$C_i^n = \frac{\omega_{fi}^n \Delta \tau}{1 + \omega_i^n \Delta \tau} \quad \text{One phase of PCM} \quad 30$$

$$C_i^n = \omega_{fi}^n \Delta \tau$$

Two phases of PCM

31

$$\omega_{fi}^n = \frac{h_{ei}^n a}{\rho_f C_f \varepsilon}$$

32

Table (1) shows the physical and thermal properties of phase change materials PCMs and heat transfer fluid HTF.

Table -1 Physical and Thermal properties of PCMs and HTF

Properties	Phase change materials						(HTF) Ethylene glycol 40% Vol
	n-tetradecane		Water		Rubitherm RT5		
	Solid	Liquid	Solid	Liquid	Solid	Liquid	
Solidifying temperature, °C	2.73	-	0	-	3	-	-
Melting temperature, °C	7.79	-	0	-	5	-	-
Solidifying latent heat, kJ/kg	213.83	-	333.6	-	196	-	-
Specific heat, kJ/kg.K	2.00	2.55	2.01	4.18	2.00	2.22	3.45
Thermal conductivity, W/m.K	0.273	0.211	2.22	0.566	0.22	2.21	0.44
Density, kg/m ³	803	765	917	1000	880	770	1070
Dynamic Viscosity, kg/m.s	-	-	-	-	-	-	0.00906

6. Results of charging process of packed bed

At this process, HTF flows in the tank from the bottom to the top of the cool TES tank. The numerical simulations are conducted at inlet temperatures (-4°C), flow rates (0.5m³/s), diameter of capsules (0.08m), Spherical capsules material is polyethylene, and the capsules filled by different type of PCMs (Water, n-tetradecane and Rubitherm).

Figure 2 shows the variation of the temperatures of PCM and HTF with time at middle ($X/L = 0.5$) and outlet positions ($X/L = 1$) of the packed bed. It is clearly seen that the PCM undergoes three stages during the charging process, namely, liquid sensible cooling stage, phase change (freezing) stage, and solid sub-cooling stage.

The PCM temperature decreases rapidly at the liquid sensible cooling stage up to the freezing temperature θ_s , and then it remains uniform at the freezing temperature until the solidification stage terminates and solid sub-cooling takes place below the freezing temperature θ_s .

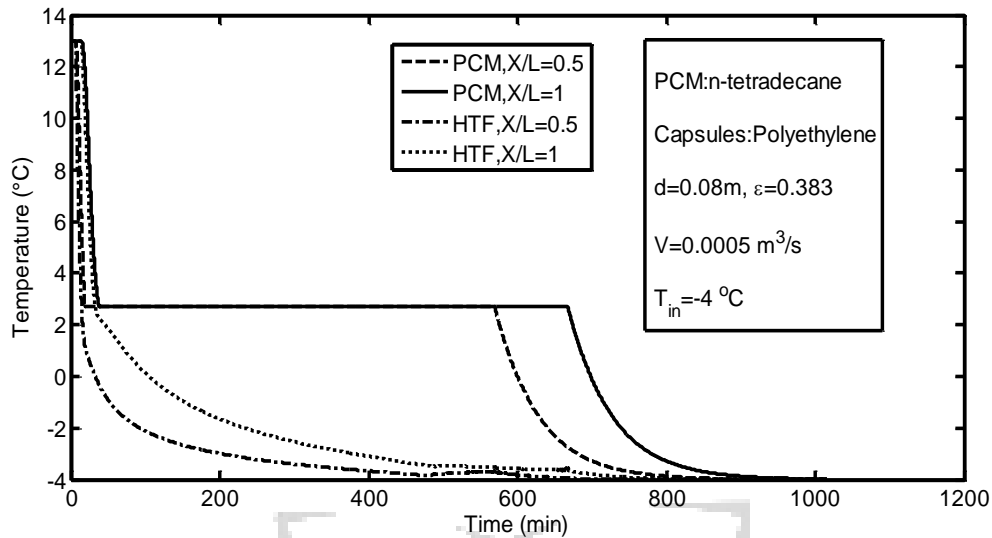


Figure 2 Temperatures distribution of PCM and HTF at middle and outlet of packed bed with time during charging process

It is also noted from Figure 2 that the HTF temperature decreases rapidly until it reaches the freezing temperature. During the freezing process, the HTF temperature decreases rapidly in the cylindrical tank at the sites near the entrance, while it decreases slowly in sites near the exit, due to the thermal resistance as a result of the layers of ice that start forming during the freezing process. The time for complete freezing at the middle location is about 569 min (9:29 hr) and at the outlet is about 667 min (11:7 hr). This is due to the fact that heat transfer rate decreases as the temperature difference between PCM and HTF decreases along the flow direction of HTF. So, it is clearly seen that the closer to the outlet position, the longer time for complete solidification and charging process. Also it is noted that the total charging time process of the system is 1015 min (16:55 hr).

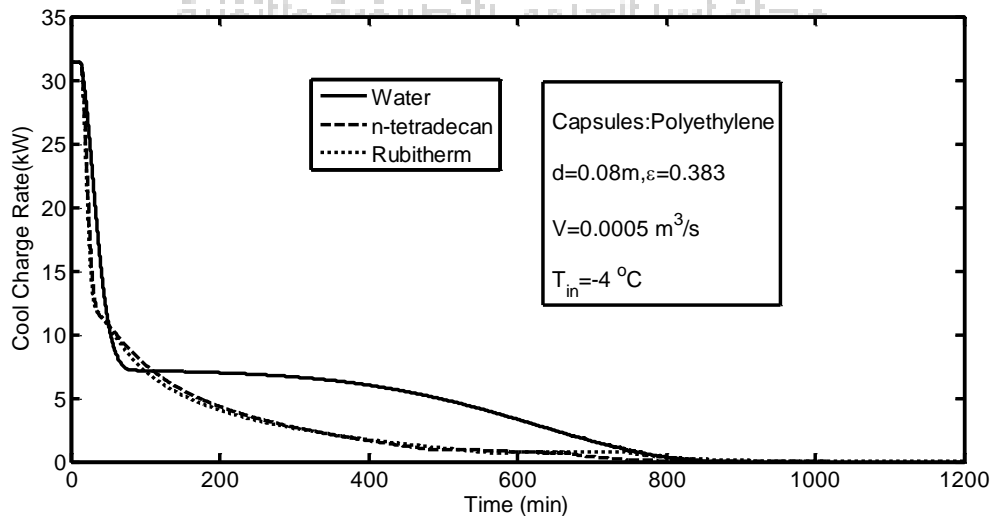


Figure 3 Variation of cool stored rate with time at different phase change materials

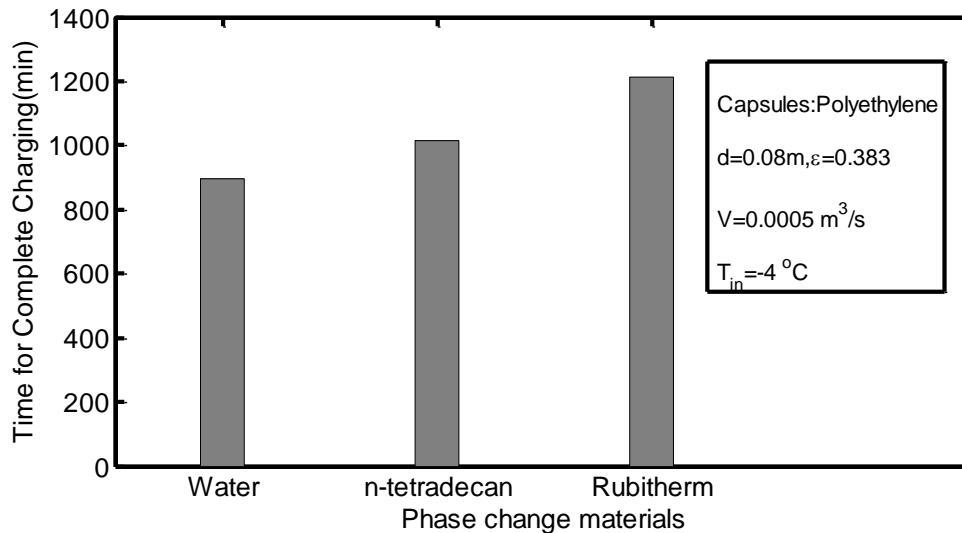


Figure 4 Effect of PCMs on time for complete charging

Figure 3 represents the variation of cool charge rate with time at different PCM, it can be observed that n- tetradecane and rubitherm charge rate decreased rapidly than water case for the liquid cooling stage, because of water high volumetric heat capacity ($\rho.c$), which is $4180 \text{ kJ/m}^3 \text{ K}$.

The volumetric heat capacity of n-tetradecane and rubitherm are 1950.75 and $1709.4 \text{ kJ/m}^3 \text{ K}$ respectively. During the freezing process, the cool charge rate of water is nearly constant at the forepart of freezing, and then it decreases slowly to zero. That is due to its higher latent heat of solidification. The latent heat of solidification of water, n-tetradecane and rubitherm are 333.6 , 213.83 and 196 kJ/kg , respectively. Higher solidifying latent heat of PCM means longer time for complete solidification.

Figure 4 displays clearly the effect of PCM on time for complete charging at different PCMs, n-tetradecane have a time for complete charging of 1015 min ($16:55 \text{ hr}$). When using water, the time for complete charging decreased to 897 min ($14:57 \text{ hr}$), by decreased percent equal to 11.6% , whereas when using rubitherm the time for complete charging increases to 1214 min ($20:14 \text{ hr}$), it is increased by 19.6% .

Figure 5 illustrates variation of cool charge capacity with time at different PCMs. It is shown that the charge capacity in water as PCM is higher than n-tetradecane and rubitherm because of its high value of volumetric heat capacity and latent heat of solidification. The cool charge capacity of water, n-tetradecane and rubitherm are 296.4 , 176 and 175.6 MJ , respectively.

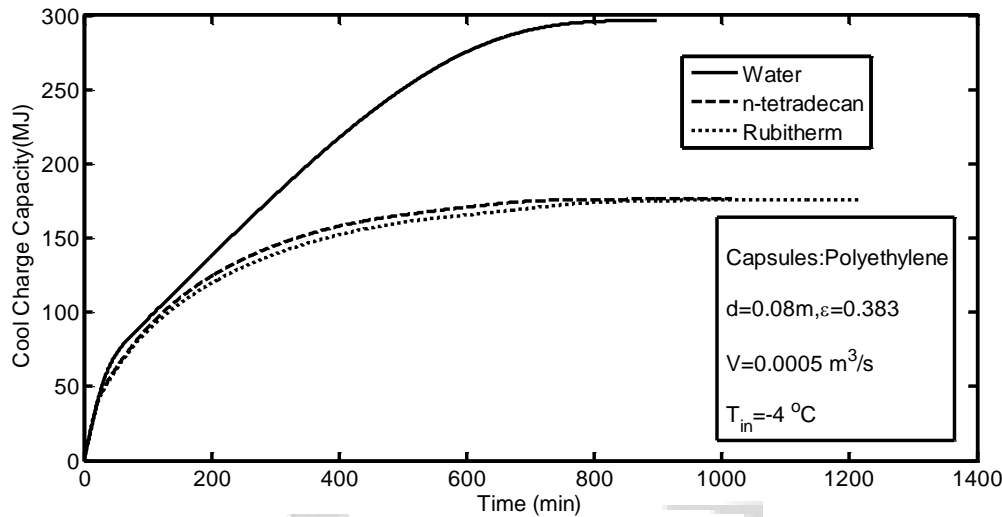


Figure 5 Variation of cool charge capacity with time at different phase change materials

6. Results of discharging process of packed bed

The flow rate of HTF, the diameter of capsules, the inlet temperature of HTF, the initial temperature of PCM and HTF, are assumed to be $0.5 \text{ m}^3/\text{s}$, 0.08 m , 13 and -4 °C, respectively.

Spherical capsules material is polyethylene, and filled by n- tetradecane as a PCM. Figure 6 displays the variation of the temperatures of PCM and HTF with time at middle and outlet positions of the packed bed during discharging process. It is clearly seen that the PCM undergoes three stages during the discharging process, namely, solid sensible heating stage, phase change (melting) stage, and liquid sensible heating stage. At the solid sensible heating stage the PCM temperature increases rapidly due to large temperature difference between HTF and solid PCM up to the melting temperature θ_m , and then it remains uniform at the melting temperature until the melting stage terminates and liquid heating takes place above the melting temperature θ_m .

It is also noted from Figure 6 that the HTF temperature increases rapidly until it reaches the melting temperature. During the melting process, the HTF temperature increases rapidly in the cylindrical tank at the sites near of the entrance, while it increases slowly in sites near of the exit. The time for complete melting at the middle location is about 895 min (14:55 hr) and at the outlet is about 1020 min (17:00 hr). This is due to the fact that heat transfer rate decreases as the temperature difference between PCM and HTF decreases along the flow direction of HTF. So, it is clearly seen that the closer to the outlet position, the longer time for complete melting and discharging process. Also note that the total discharging time process of the system is 1466 min (24:26 hr).

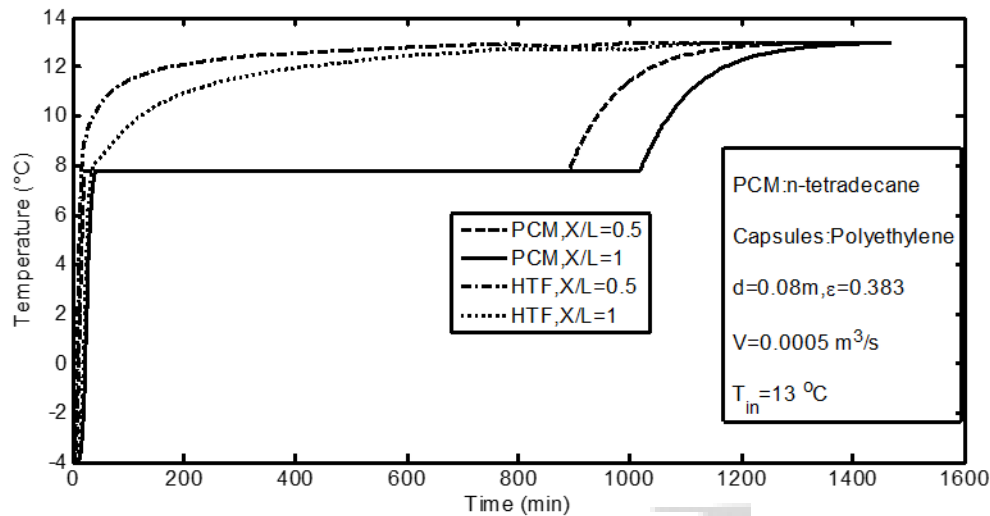


Figure 6 Temperatures distribution of PCM and HTF at middle and outlet of packed bed with time during discharging process

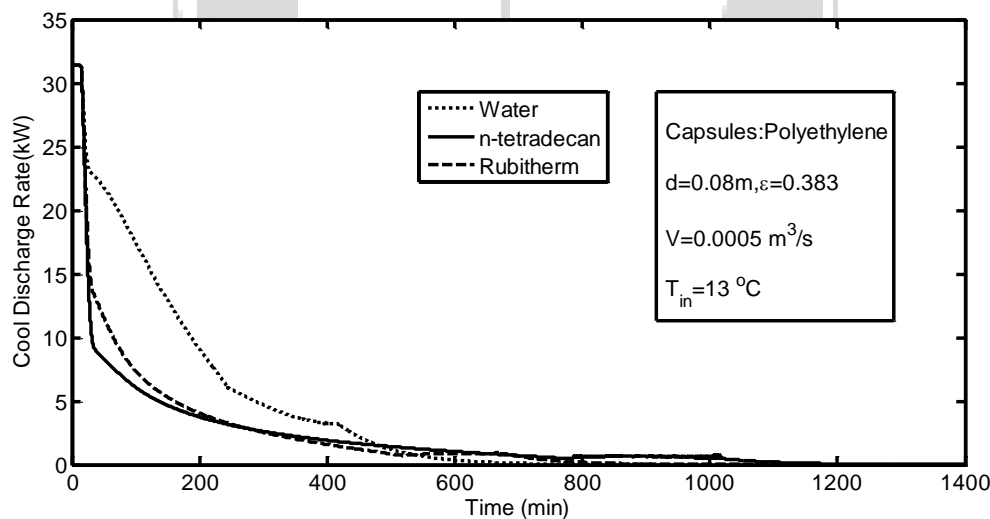


Figure 7 Variation of cool discharge rate with time at different phase change materials

Figure 7 represents the variation of cool discharge rate with time at different PCM, it can be observed that n-tetradecane and rubitherm discharge rate decreased rapidly than water case for the solid heating stage, because of water high volumetric heat capacity ($\rho.c$), which is $1843 \text{ kJ/m}^3 \text{ K}$. The volumetric heat capacity of n-tetradecane and rubitherm are 1606 and $1760 \text{ kJ/m}^3 \text{ K}$ respectively. Figure 8 displayed clearly the effect of PCM on time for complete discharging at different PCMs. It is clearly seen that the longer time for complete charging process. Times for complete discharging of water, rubitherm, and n-tetradecane are 910, 1111, 1466 min, respectively

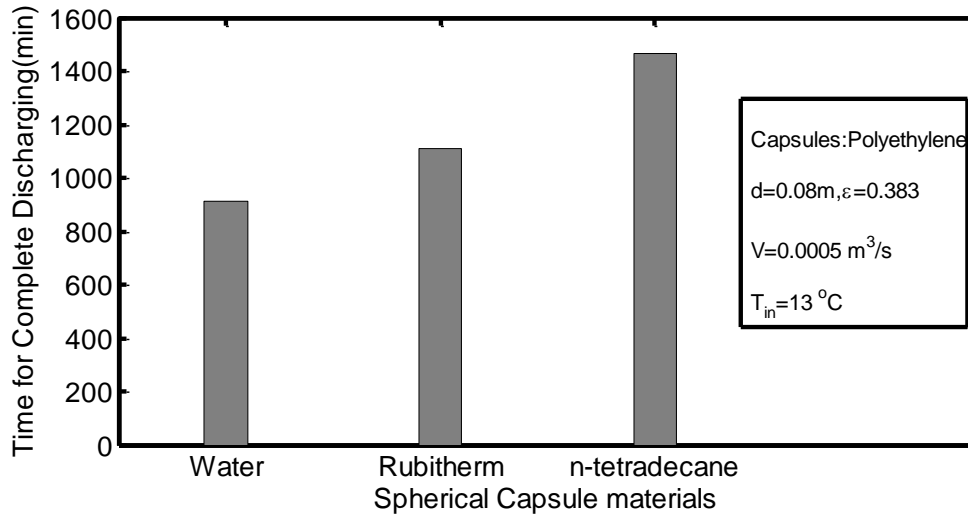


Figure 8 Effect of PCMs on time for complete discharging

Figure 9 illustrates variation of cool discharge capacity with time at different PCMs.

It is shown that the discharge capacity in water as PCM is higher than n-tetradecane and rubitherm because of its high value of volumetric heat capacity and latent heat. The cool discharge capacity of water, n-tetradecane and rubitherm are 296, 174 and 175 MJ, respectively.

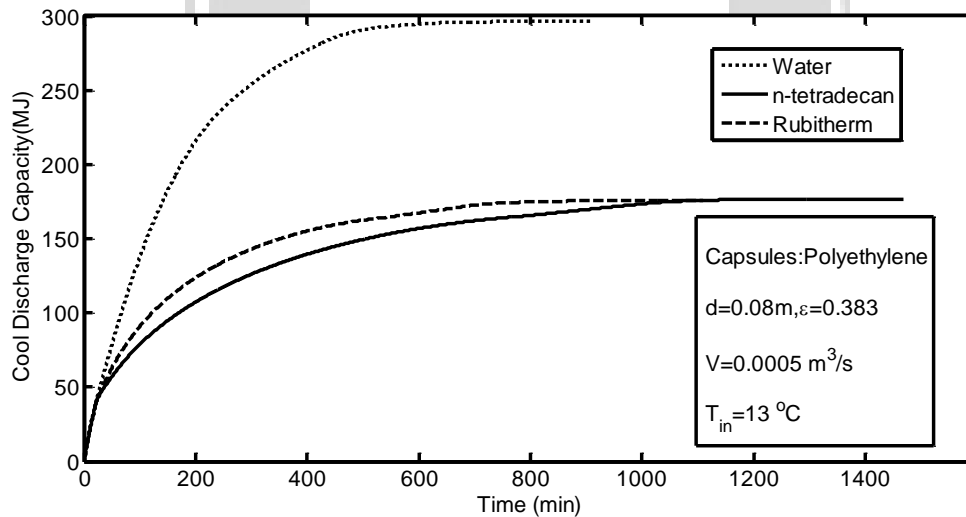


Figure 9 Variation of cool discharge capacity with time at different phase change materials

7. Conclusion

The time for complete charging and discharging is low with PCM which has high volumetric heat capacity and high thermal conductivity. Time for complete discharging was longer than the time of complete charging process at the case of n-tetradecane as PCM, which are 1015 min for charge and 1466 min for discharge, as a reason of the lower heat transfer coefficient.

References

- [1] K.A.R. Ismail, J.R. Henriquez, "Numerical and experimental study of spherical capsules packed bed latent heat storage system," *Applied Thermal Engineering*, vol. 22, pp. 1705-1716, 2002.
- [2] L. Bilir, Z. Ilken, "Total solidification time of a liquid phase change material enclosed in cylindrical/spherical containers," *Applied Thermal Engineering*, vol. 25, pp. 1488-1502, 2005.
- [3] Regin A. Felix, Solanki S.C., and Saini J.S, "An analysis of a packed bed latent heat thermal energy storage system using PCM capsules: Numerical investigation," *Renewable Energy*, vol. 34, pp. 1765-1773, 2009.
- [4] Shuangmao Wu, Guiyin Fang, Xu Liu, "Thermal performance simulations of a packed bed cool thermal energy storage system using n-tetradecane as phase change material," *International Journal of Thermal Sciences*, vol. 49, pp. 1752-1762, 2010.
- [5] M. Cheralathan, R. Velraj, S. Renganayanan, "Effect of porosity and inlet heat transfer fluid temperature variation on the performance of cool thermal energy storage system," *Heat and Mass Transfer*, vol. 43, pp. 833-842, 2007.
- [6] Reda I. ElGhnam, Ramdan A. Abdelaziz, Mohamed H. Sakr, Hany E. Abdelrhman, "An experimental study of freezing and melting of water inside spherical capsules used in thermal energy storage systems," *Ain Shams Engineering Journal*, vol. 3, pp. 33-48, 2012.
- [7] Cho K, Choi SH, "Thermal characteristics of paraffin in a spherical capsule during freezing and melting processes," *Heat and Mass Transfer*, vol. 43, pp. 3183-3196, 2000.
- [8] S. Ergun, "Chemical Engineering Progress," p. 48, 1952.
- [9] G.J. Beavers, E.M. Sparrow, D.E. Rodenz, "Influence of bed size on the flow characteristics and porosity of randomly packed bed of spheres," *J. Appl. Mech*, vol. 40, p. 655, 1973.
- [10] J.Beek, "Design of packed catalytic reactor," *Advanced in Chemical Engineering*, *Advanced in Chemical Engineering*, vol. 3, pp. 203-271, 1962.